J. Biochem. **140**, 763–776 (2006)
doi:10.1093/jb/mvj210

The Amino-Terminus of Mouse DNA Methyltransferase 1 Forms an Independent Domain and Binds to DNA with the Sequence Involving PCNA Binding Motif

Isao Suetake*, Daichika Hayata and Shoji Tajima
Institute for Protein Research, Osaka University, 3-2 Yamadaoka, Suita, Osaka 565-0871

Received July 19, 2006; accepted September 7, 2006

DNA methylation patterns in genome are maintained during replication by a DNA methyltransferase Dnmt1. Mouse Dnmt1 is a 180 kDa protein comprising the N-terminal regulatory domain, which covers 2/3 of the molecule, and the rest C-terminal catalytic domain. In the present study, we demonstrated that the limited digestion of full-length Dnmt1 with different proteases produced a common N-terminal fragment, which migrated along with Dnmt1 (1–248) in SDS–polyacrylamide gel electrophoresis. Digestion of the N-terminal domains larger than Dnmt1 (1–248) with chymotrypsin again produced the fragment identical to the size of Dnmt1 (1–248). These results indicate that the N-terminal domain of 1–248 forms an independent domain. This N-terminal domain showed DNA binding activity, and the responsible sequence was narrowed to the 79 amino acid residues involving the proliferating cell nuclear antigen (PCNA) binding motif. The DNA binding activity did not distinguish between DNA methylated and non-methylated states, but preferred to bind to the minor groove of AT-rich sequence. The DNA binding activity of the N-terminal domain competed with the PCNA binding. We propose that DNA binding activity of the N-terminal domain contributes to the localization of Dnmt1 to AT-rich sequence such as Line 1, satellite, and the promoter of tissue-specific silent genes.

Key words: DNA binding, DNA methylation, DNA methyltransferase, domain structure, proliferating cell nuclear antigen.

Abbreviations: CBB, Coomassie Brilliant Blue R-250; DAPI, 4′,6-diamidino-2 phenylindole; DTT, dithiothreitol; HDAC, histone deacetylase; PCNA, proliferating cell nuclear antigen.

In vertebrates, the 5th positions of cytosine residues in CG sequences in genomic DNA are often methylated (*1*, *2*). DNA methylation plays crucial roles in development (*3*) and a variety of biological processes, such as genomic imprinting (*4*) and carcinogenesis (*5*) *via* suppression of certain genes (*6*). In vertebrates, two types of DNA methyltransferase activities have been reported, *i.e., de novo* and maintenance types. In mouse, *de novo* type DNA methylation creates tissue-specific methylation patterns at the implantation stage (*7*), and maintenance type methylation ensures clonal transmission of gene-specific methylation patterns during replication.

One of the DNA methyltransferases, Dnmt1, is responsible for the latter activity. Dnmt1 localizes to replication fork at S-phase and interact with replication machinery through proliferating cell nuclear antigen (PCNA) to methylate the newly synthesized hemi-methylated DNA to maintain the methylation patterns (*8–11*). In addition, Dnmt1 is recruited to the repair lesion with PCNA, playing a role in maintaining the methylation patterns after repair (*12*). Targeting of Dnmt1 gene results in global demethylation of genome and consequently causes death at early stage of embryogenesis (*13*). Mouse Dnmt1 is composed of 1,620 amino acid residues and 1/3 of them at the C-terminus encode the sequences conserved among the DNA (cytosine-5) methyltransferase family (*14*). The large N-terminal and the C-terminal catalytic parts are separated with a $(KG)_{5\text{-}7}$ repeat (*15–19*). This large N-terminal region is thought to be a regulatory region contributes to the recognition of hemi-methylated DNA (*14*), and interacts with several functional proteins such as transcription factor DMAP1 (*20*), PCNA (*9*), histone deacetylase (HDAC) (*20*,*21*), oncoprotein Rb (*22*, *23*), methylated DNA binding protein MeCP2 (*24*), heterochromatin binding protein 1 (HP1) (*25*), p53 (*26*), and *de novo*–type DNA methyltransferases DNMT3a and DNMT3b (*27*).

Margot *et al.* proposed to divide further the above large N-terminal region into two regions, which are 1–353 and the rest, judging from intron/exon size and exon arrangement (*28*). The N-terminus 1–353 contains the sequences interacting with DMAP1, HDAC2, PCNA, Rb, MeCP2, Dnmt3a, and Dnmt3b (*9*, *20*, *23*, *24*, *27*). It was also reported that this N-terminal region has DNA binding activity (*29–31*). Araujo *et al.* reported that human Dnmt1 fragment 122–417 contains the region for the recognition of hemi-methylated DNA (*30*). However, Fatemi et al. reported that the mouse Dnmt1 1–343 is not involved in the recognition of hemi-methylated DNA (*29*). Consistent with the report by Fatemi *et al.*, we have reported

*To whom correspondence should be addressed. Phone: +81-6-6879-8628, Fax: +81-6-6879-8629, E-mail: suetake@protein.osaka-u.ac.jp

that the N-terminal region 1–290 is dispensable for the hemi-methylated DNA methylating activity (*32*).

In the present study, we demonstrated that limited proteolysis of Dnmt1 with different proteases commonly produced a fragment derived from the N-terminus, of which size was identical to the sequence 1–248. Thus we estimated that the N-terminal 1–248 forms an independently folded domain. In addition, we narrowed the responsive sequence for the DNA binding activity to 119–197 of the N-terminal domain. This DNA binding activity preferred to bind to the minor groove of AT-rich sequence. Interestingly, the sequence responsible for the DNA binding partly overlapped with the PCNA binding motif, and thus the binding of Dnmt1 to DNA competed with PCNA.

MATERIALS AND METHODS

Plasmid Construction—The 5′-end cDNA encoding the somatic type Dnmt1 1–118 was kindly provided by Heinrich Leonhardt at Ludwig Maximilians University, Munich, Germany. The truncated and mutated cDNAs encoding the N-terminal regions of Dnmt1 were PCR-amplified with recombinant Taq DNA polymerase (Toyobo, Tokyo), and then subcloned into pGEX6P-1 (GE Healthcare Bio-Sciences) or pET22b (Novagen). The amino acid sequence of His-tagged Dnmt1 N-terminal region was constructed to be identical to those corresponding to His-tagged full-length Dnmt1 (*32*). The cDNAs of PCNA, wild type and two mutants that cannot bind to DNA (*33*), kindly provided by Toshiki Tsurimoto at Kyushu University, Kyushu, Japan, were subcloned into pET23a (Novagen). The nucleotide sequences of the cDNAs were verified by the dideoxy methods (*34*).

Recombinant Protein Expression and Purification—His-tagged full-length Dnmt1 was expressed in Sf9 cells and purified as described elsewhere (*32*). All the N-terminal constructs of Dnmt1 with GST- and His-tags, and His-tagged PCNA were expressed in BL21-Codon Plus-RIL (Stratagene, CA) at 18°C with 0.5 mM isopropyl-1-thio-β-galactoside treatment. The expressed proteins were purified using glutathione-Sepharose (GE Healthcare Bio-Sciences) as described (*35*). His-tagged PCNA was purified with a HiTrap chelating Sepharose HP column (GE Healthcare Bio-Sciences) according to the manufacturer's instruction, and then dialyzed against a buffer comprising 0.1 M NaCl, 1 mM EDTA, 10% (v/v) glycerol, 0.01% (w/v) Triton X-100, 1 mM dithiothreitol (DTT), and 25 mM Hepes (pH 7.9). Protein concentrations were determined by BCA assay kit (Pierce, IL) using bovine serum albumin as a standard.

Limited Proteolysis of Dnmt1—Dnmt1 was treated with indicated amounts of chymotrypsin type II (Sigma, MO), V8 (Wako, Osaka), or TPCK-Trypsin (Pierce), at 25°C in a reaction buffer comprising 0.5 M NaCl, 0.5 mM EDTA, 10 mM Tris-HCl (pH 7.4). Unless otherwise mentioned, after an hour incubation, the reaction was terminated by adding protease inhibitor cocktail (Nakalai Tesque, Kyoto), and were separated in a 10% SDS–polyacrylamide gel.

SDS–Polyacrylamide Gel Electrophoresis and Western Blotting—Proteins were subjected to SDS–polyacrylamide gel electrophoresis (*36*), and stained with Coomassie Brilliant Blue R-250 (CBB). For Western blotting, protein bands were electrophoretically transferred to PVDF (Millipore) or nitrocellulose membranes (Schleicher & Schuell) after the electrophoresis. The membranes were blocked and immuno-stained with polyclonal anti His-tag antibodies (MBL, Nagoya).

Table 1. **Sequences of the oligonucleotide DNA used for gel shift analyses.**

Name	Sequences
26CG	5′-GCCTCCTTGGCTGACGTCAGAGAGAG-3′
	3′–CGGAGGAACCGACTGCAGTCTCTCTC-5′
26CA	5′-GCCTCCTTGGCTGACATCAGAGAGAG-3′
	3′-CGGAGGAACCGACTGTAGTCTCTCTC-5′
26AT	5′-GATTATTTAACTGATTTCATAAATAG-3′
	3′-CTAATAAATTGACTAAAGTATTTATC-5′
42U	5′-GATCCGACGACGACGACGACGACGACGA-CGACGACGACGATC-3′
	3′-CTAGGCTGCTGCTGCTGCTGCTGCTGCTG-CTGCTGCTGCTAG-5′
42H1	5′-GATCMGAMGAMGAMGAMGAMGAMGAM-GAMGAMGAMGAMGATC-3′
	3′-CTAGGCTGCTGCTGCTGCTGCTGCTGCTG-CTGCTGCTGCTAG-5′
42H2	5′-GATCGTCGTCGTCGTCGTCGTCGTCGTCG-TCGTCGTCGGATC-3′
	3′-CTAGMAGMAGMAGMAGMAGMAGMAGM-AGMAGMAGMAGMCTAG-5′
42M	5′-GATCMGAMGAMGAMGAMGAMGAMGAM-GAMGAMGAMGAMGATC-3′
	3′-CTAGGMTGMTGMTGMTGMTGMTGMTG-MTGMTGMTGMTGMTAG-5′
27U	5′-TCAGACCACGTGGTCGGGTGTTCCTGA-3′
	3′-AGTCTGGTGCACCAGCCCACAAGGACT-5′

M denotes 5-methyl deoxycytosine. CpG sequence is indicated by underlines.

Gel Shift Assay—The oligonucleotide DNAs used for gel-shift assay are summarized in Table 1. The synthesized complementary oligonucleotides were annealed and then used for gel shift assay. Double-stranded DNA (2 pmol), of which the 5′-end was labeled with [γ-^{32}P]-ATP (GE Healthcare Bio-Sciences) and T4 polynucleotide kinase (Toyobo) in some of the experiments, was incubated with a series of truncated proteins (5 pmol) at 30°C for 30 min in 25 μl of a solution comprising 20 mM NaCl, 1 mM EDTA, 10% (v/v) glycerol, 1 mM DTT, 1/1,000 (v/v) protease inhibitor cocktail, and 50 mM Tris-HCl (pH 7.6), and then the mixture was subjected to electrophoresis in a 0.7% agarose gel with 1× TBE. The ^{32}P-labeled DNA was determined by exposing the dried gel to X-ray film and the radioactivity of the shifted band was quantitated by exposing to an imaging plate (Fuji Photo Film) (*37*). The non-labeled DNA was stained with SYBR Green I (Invitrogen) and determined in a FluoroImager as described (*35*).

The minor groove binding agents, distamycin A (Sigma), 4′,6-diamidino-2-phenylindole (DAPI) (Nakalai Tesque), or netropsin (Sigma), or the major groove binding agent, methyl green (Nakalai Tesque), was preincubated with annealed oligonucleotide, 26AT or 26CG, at room temperature for 15 min. After the preincubation, recombinant Dnmt1 was added and further incubated at 30°C for 30 min. The mixture was subjected to electrophoresis and analyzed as described above.

For the competition assay, 5 pmol of Dnmt1 was mixed with 2 pmol of radio-labeled oligonucleotide, of which the

5′-end was labeled with ^{32}P, and indicated amounts of unlabeled oligonucleotide, and then incubated at 30°C for 30 min. The reaction mixture was subjected to a 6% polyacrylamide gel or a 0.7% agarose gel with a 1× TBE buffer, and the shifted bands were determined as described above.

Nitrocellulose Filter Binding Assay—Double-stranded oligonucleotide (2 pmol) radio-labeled at the 5′ end with ^{32}P was incubated with 5 pmol of GST-Dnmt1 (119–197) under identical conditions described in the "gel-shift assay" section, except that the 50 μg/ml bovine serum albumin was added to the incubation mixture. The filter binding assay was performed as described by Fatemi *et al.* (*29*) with a modification. The GST-Dnmt1 (119–197)-bound nitrocellulose membranes were washed with 50 mM Tris-HCl (pH 7.5), 20 mM NaCl, 1 mM EDTA, 10% (w/w) glycerol. The radioactivity remained on the membranes was determined with a BAS2000 (Fuji Photo Film).

Pull Down Assay—GST-Dnmt1 (119–197) (60 pmol) bound to glutathione-Sepharose was incubated with His-tagged PCNA (60 pmol), wild-type or mutants that cannot bind to DNA (*33*), in the absence or presence of 180 or 600 pmol of annealed oligonucleotide, 26CG, in a 300 μl reaction mixture comprising 0.1 M NaCl, 10% (v/v) glycerol, 0.01% (w/v) NP-40, 1 mM DTT, 1/1,000 (v/v) protease inhibitors cocktail, and 25 mM Tris-HCl (pH 7.5) as described (*35*). After the incubation at 30°C for 30 min, the matrices were washed four times with the binding buffer. Equivalent amount of total, unbound, and bound fractions were loaded onto a 12% SDS–polyacrylamide gel. The GST-Dnmt1 (119–197) and His-tagged PCNA bands were determined by immuno-blotting with anti-GST antibodies (*35*) and anti His-tag antibodies, respectively.

RESULTS

N-Terminal Region of Dnmt1 Forms a Domain Structure—Margot *et al.* reported that the large N-terminal domain of Dnmt1, which is more than 100 kDa and constitutes almost 2/3 of the molecule, can be divided into two parts from the analyses of the exon-intron arrangements and the nucleotide sequence homology among several species. Mouse Dnmt1 can be divided into the N-terminus domain comprising 353 amino acid residues and the rest that contains indispensable region for the expression of DNA methylation activity (*28*). We expected that if the N-terminal domain structure proposed by Margot *et al.* forms an independently folded domain, the N-terminal domain of Dnmt1 could be protected from protease digestion. To examine if this is the case, the purified recombinant full-length Dnmt1 was digested with chymotrypsin (Fig. 1A). When Dnmt1, which had His-tag and 24 amino acid residues at the N-terminus as extra sequences, was digested with increasing concentrations of chymotrypsin, a band migrated to an apparent position of 36 kDa was produced at a low chymotrypsin concentration, 1/1,000 (w/w) of Dnmt1 (Fig. 1A, lane 3). The anti His-tag antibodies immuno-detected this 36 kDa band as well as the intact size Dnmt1, which is about 180 kDa (Fig. 1A, lanes 6–8). In addition, the antibodies against the N-terminal sequence (1–118) (*38*) also immuno-reacted with the 36 kDa band (data not shown). The results clearly indicate that the 36 kDa band is derived from the N-terminus. The 36 kDa band was detected even after 8 h incubation with a low chymotrypsin concentration, which was 1/1,000 (w/w) of Dnmt1 (Fig. 1B).

This N-terminus derived 36 kDa band was also detected by V8 protease, trypsin (Fig. 1C), and thermolysin (supplementary figure S1) digestions. V8 protease at 1/100 (w/w) Dnmt1 wiped out intact 180 kDa Dnmt1 while the 36 kDa band remained (Fig. 1C, lane 4). The results that an almost identical size 36 kDa fragment derived from the N-terminus was produced by different proteases indicate that this N-terminal 36 kDa sequence forms a domain structure. When the recombinants of His-tagged N-terminal Dnmt1 of 1–290 (exon 1–11) and 1–317 (exon 1–12), which migrated slower than the 36 kDa band, were digested with chymotrypsin, the 36 kDa band was produced shortly after the treatment and accumulated during the digestion (Fig. 1D). This further supports that the N-terminal 36 kDa sequence stably exist as an independent domain.

In addition to the 36 kDa band, a 22 kDa size band was detected by the digestion with chymotrypsin, trypsin, and thermolysin (Fig. 1B, lane 5, Fig. 1C, lane 8, and supplementary figure S1). The production of 22 kDa band seemed to follow that of 36 kDa band. This precursor-product relationship was clear when the recombinant N-terminal Dnmt1 sequences were digested (see Fig. 1D). Thus the results suggest that the 22 kDa band at the N-terminus forms sub-domain structure. Judging from the molecular mass, this 22 kDa fragment contains 1–118, which is lacking in mammalian oocyte-type Dnmt1 (*39*). This region possesses a typical coiled-coil sequence and conserved among the species (*40*). It was reported that the V8 protease digests near the (KG)-repeat of Dnmt1 and produces the 58 kDa C-terminus catalytic domain (*14*). The 58 kDa band appeared after the 36 kDa band disappeared (data not shown). The partial N-terminal sequence of this 58 kDa band was identical to that reported by Bestor (*14*). The hinge between the 36 kDa N-terminus domains and the rest seems to be more susceptible to the proteolysis than the hinge connecting the C-terminal catalytic domain and the middle part of the molecule.

To estimate the cleavage site to produce N-terminal domain, we next prepared the partial sequences of the N-terminal region with the His-tag and extra sequences identical to that of the full-length Dnmt1, and compared their sizes with the chymotrypsin digest of the full-length Dnmt1 in SDS–polyacrylamide gel electrophoresis (Fig. 1E). As shown in Fig. 1E, the mobility of the recombinant of the Dnmt1 (1–248), which is the product of exon 1–9, seemed to be identical with that of the N-terminal 36 kDa band (see lanes 4, 8–10). This indicates that the cleavage site by chymotrypsin was at or near the amino acid number 248.

N-Terminal Domain of Dnmt1 Possesses DNA Binding Activity—It was reported that the N-terminal region of Dnmt1 has DNA binding activity (*29–31*). Fatemi et al. have reported that mouse Dnmt1 (1–343) possesses CG dinucleotide-specific DNA binding activity (*29*). To examine whether or not the N-terminal 1–248 domain contains the CG-specific DNA binding activity reported by Fatemi, GST-fused Dnmt1 (1–248) [GST-Dnmt1 (1–248)] and GST-Dnmt1 (1–343) were purified (Fig. 2A), and then

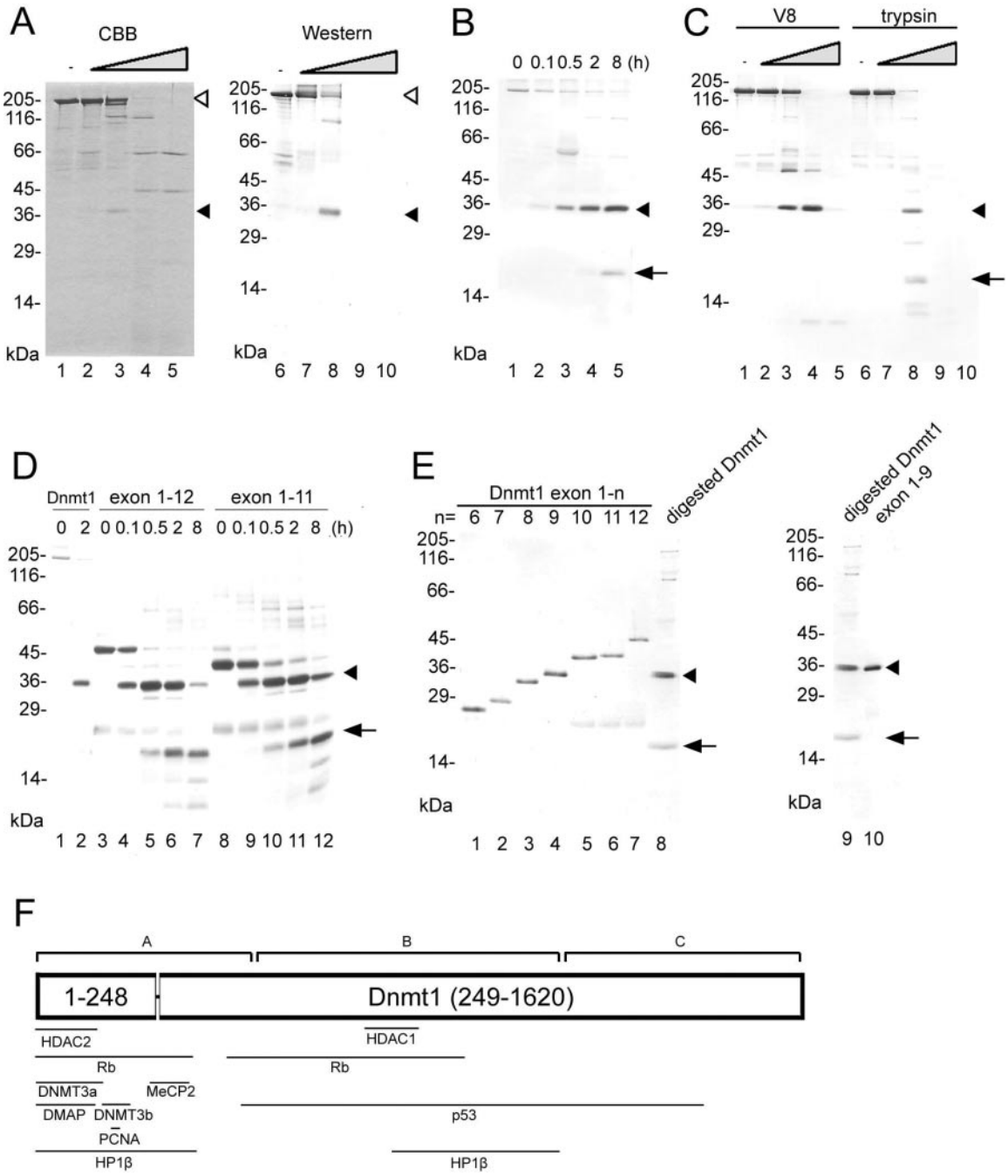

Fig. 1. **Core domain in the N-terminus of Dnmt1.** (A) Dnmt1 was digested with increasing concentrations of chymotrypsin. Fixed amount of Dnmt1 (10 μg) (lanes 1 and 6) was digested with 1/10,000 (lanes 2 and 7), 1/1,000 (lanes 3 and 8), 1/100 (lanes 4 and 9), and 1/10 (lanes 5 and 10) (w/w Dnmt1) of chymotrypsin for 1 h. (B) Dnmt1 (10 μg) (lane 1) was digested with 1/1,000 (w/w Dnmt1) chymotrypsin for 6 min (lane 2), 30 min (lane 3), 2 h (lane 4), and 8 h (lane 5). (C) Dnmt1 was digested with increasing concentrations of V8 (lanes 1–5) and TPCK-trypsin (trypsin) (lanes 6-10). Dnmt1 (10 μg) (lanes 1 and 6) was digested with 1/10,000 (lanes 2 and 7), 1/1,000 (lanes 3 and 8), 1/100 (lanes 4 and 9), and 1/10 (lanes 5 and 10) (w/w Dnmt1) for 1 h. (D) Dnmt1 (1–317) (exon 1–12, lanes 3–7), (1–290) (exon 1–11, lanes 8–12), and purified full-length Dnmt1 (lanes 1 and 2) (10 μg protein each) were digested with 1/1,000 (w/w) of chymotrypsin for 0 min (lanes 1, 3, and 8), 6 min (lanes 4 and 9), 30 min (lanes 5 and 10), 2 h (lanes 2, 6, and 11), and 8 h (lanes 7 and 12). (E) Dnmt1 (1–197) (exon 1–6, lane 1), (1–208) (exon 1–7, lane 2), (1–234) (exon 1–8, lane 3), (1–248) (exon 1–9, lanes 4 and 10), (1–276) (exon 1–10, lane 5), (1–290) (exon 1–11, lane 6), and (1–317) (exon 1–12, lane 7) were expressed as fusion with the identical His-tag and extra sequences to that of full-length Dnmt1 at N-terminus, and purified with chelating-Sepharose. The panels indicate Western blotting of the purified proteins and full-length Dnmt1 digested with 1/1,000 (w/w Dnmt1) of chymotrypsin for 1 h (lanes 8 and 9). All the mixtures were electrophoresed in 12% SDS-polyacrylamide gels, and protein bands were stained with CBB (panel A left), or immuno-stained with anti His-tag antibodies (panels A right and B-E). Open and closed arrowheads and arrows indicate the positions of full-length Dnmt1, the N-terminal 36 kDa, and 22 kDa fragments, respectively. (F) The N-terminal domain of Dnmt1 (1–248) identified in the present study is schematically illustrated. The tripartite structure predicted by Margot et al. is shown as domain A, B, and C (*28*), and the interacting sites with various functional proteins are indicated with underlines.

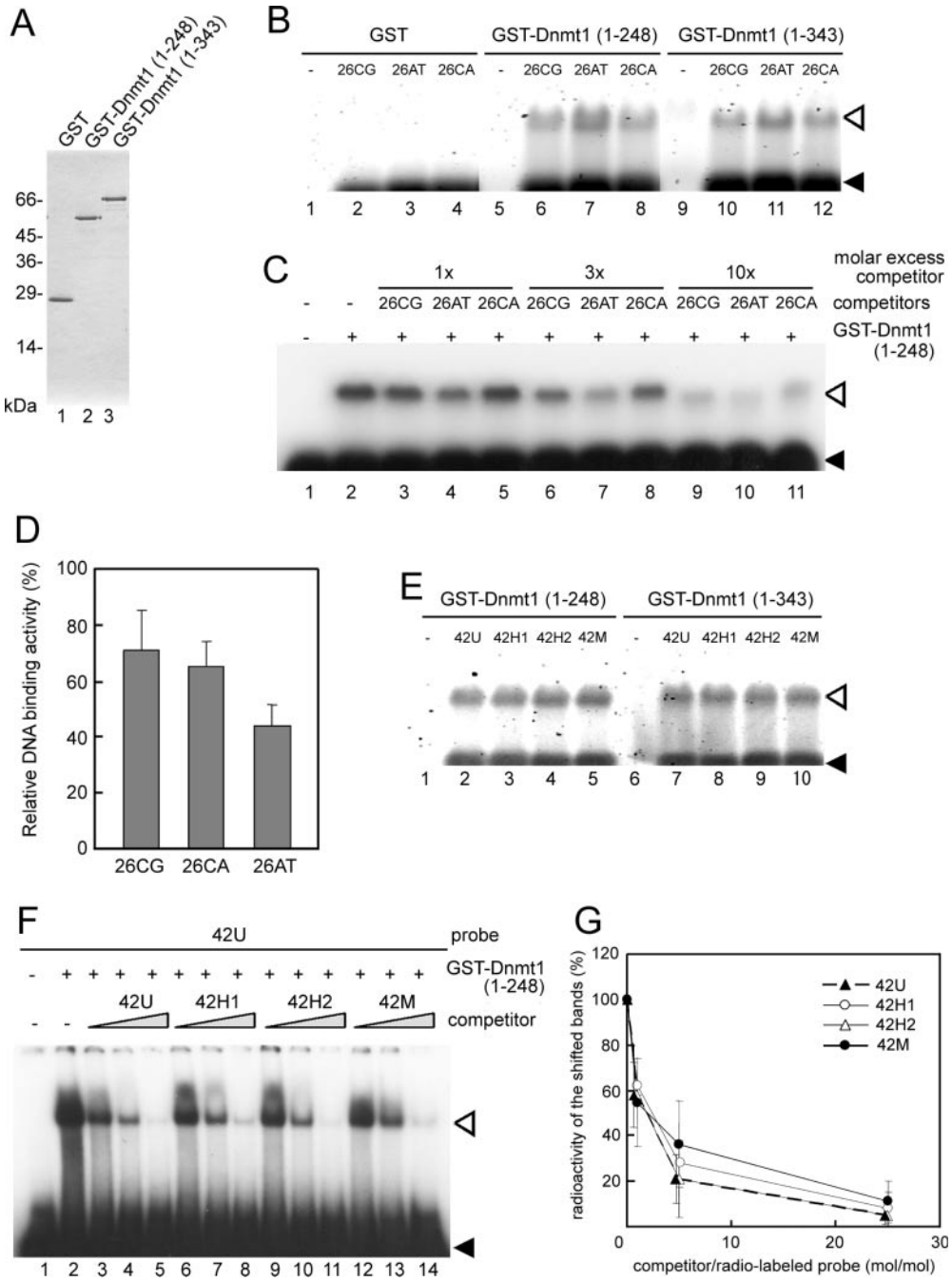

Fig. 2. **DNA binding activity of the N-terminal domain of Dnmt1.** (A) GST (lane 1), GST-Dnmt1 (1–248) (lane 2), and GST-Dnmt1 (1–343) (lane 3) (2 μg protein each) were electrophoresed in a 12% SDS–polyacrylamide gel, and protein bands were stained with CBB. (B) GST (lanes 1–4), GST-Dnmt1 (1–248) (lanes 5–8), or GST-Dnmt1 (1–343) (lanes 9–12) was incubated without probe, with 26CG, 26CA, or 26AT (Table 1). The mixtures were electrophoresed in a 0.7% agarose gel with a 1× TBE buffer. DNA was visualized with SYBR green I. (C) Radio-labeled 26AT was incubated without (lane 1) or with (lanes 2–11) GST-Dnmt1 (1–248), and no (lanes 1 and 2), one (lanes 3–5), three (lanes 6–8), or ten (lanes 9–11) molar excess non-labeled 26CG (lanes 3, 6, and 9), 26AT (lanes 4, 7, and 10), or 26CA (lanes 5, 8, and 11). The mixtures were electrophoresed as in B, and exposed to X-ray film. (D) Radio-labeled 26AT and three molar excess of cold 26CG, 26AT, or 26CA were incubated and electrophoresed as in C. The radioactivity of the shifted bands were determined by a BAS2000 and plotted. The average values ± SD were calculated from five independent experiments. (E) GST-Dnmt1 (1–248) (lanes 1–5) or GST-Dnmt1 (1–343) (lanes 6–10) was incubated without probe (lanes 1 and 6), with 42U (lanes 2 and 7), 42H1 (lanes 3 and 8), 42H2 (lanes 4 and 9), or 42M (lanes 5 and 10) probe (see Table I) as in (B). (F) Radio-labeled 42U was incubated without protein (lane 1), or with GST-Dnmt1 (1–248) (lanes 2–14), and then was chased with 1, 5, and 25 molar excess of 42U (lanes 3–5), 42H1 (lanes 6–8), 42H2 (lanes 9–11), or 42M (lanes 12–14) as competitor. After the incubation, the reaction mixtures were electrophoresed in a 6% polyacrylamide gel with a 1× TBE buffer, and the gel was subjected to autoradiography. (B, C, E, and F) Open and closed arrowheads indicate the positions of the shifted bands and free probes, respectively. (G) Quantitative analysis of panel F. The radioactivity in the shifted bands from five independent experiments was determined, normalized to the radioactivity of the shifted bands without competitors, and the average ± SD was plotted.

determined their DNA binding activity. For the binding experiment, 26 bp double-stranded DNAs containing one CG/GC (26CG), this CG/GC changed to CA/GT (26CA), and AT-rich (26AT) sequences were used (Table 1). GST-Dnmt1 (1–248) bound to 26CG in a similar level to that of GST-Dnmt1 (1–343) (Fig. 2B, compare lanes 6 and 10). In addition, GST-Dnmt1 (1–248) and GST-Dnmt1 (1–343) bound to 26CA, which does not contain CG sequence, to a similar level as that to 26CG (Fig. 2B, compare lanes 6, 8, 10, and 12). Interestingly, GST-Dnmt1 (1–248) as well as GST-Dnmt1 (1–343) showed higher binding activity for 26AT, of which sequence was AT-rich and contains no CG sequence (Fig. 2B, lanes 7 and 11). The radio-labeled 26AT DNA bound to GST-Dnmt1 (1–248) was efficiently competed by the addition of cold 26AT than 26CG or 26CA (Fig. 2, C and D), supporting that this N-terminal domain preferentially binds to AT-rich sequence. Different from the report by Fatemi *et al.* (*29*), the DNA binding activity of the N-terminal domain did not show any strong preference for the CG sequence but it preferred to bind AT-rich sequence. Since the DNA binding specificity of GST-Dnmt1 (1–248) was identical to that of GST-Dnmt1 (1–343) (Fig. 2B), the sequence of Dnmt1 (249–343) may not be involved in the DNA binding activity and its specificity.

The specificity of the methylated DNA binding activity of the N-terminal domain is rather controversial. One report argues that the sequence of human Dnmt1 122–417 including PCNA binding motif specifically recognizes hemi-methylated DNA (*30*). On the other hand, it was reported that the N-terminal domain (1–343) does not discriminate methylated and unmethylated DNA, but rest of the regions 613–748 and 1124–1620 are responsible for the recognition of hemi-methylated DNA (*29*). Recently, we have reported that the N-terminal domain is dispensable for the preferential methylation of hemi-methylated DNA (*32*).

To determine the DNA binding specificity of the N-terminal 1–248, we examined the DNA binding activity of GST-Dnmt1 (1–248) towards non-methylated, hemi-methylated, fully methylated DNA, of which sequences are shown in Table 1. Similar to the N-terminal DNA binding domain reported by Fatemi *et al.* (*29*), the GST-Dnmt1 (1–248) and GST-Dnmt1 (1–343) could not discriminate unmethylated (42U), hemi-methylated (42H1 and 42H2), and fully methylated (42M) double-stranded 42-bp DNA containing 12 pairs of CpG sequences (Fig. 2E). Furthermore, the unmethylated DNA bound to GST-Dnmt1 (1–248) was equally competed by the addition of the unmethylated, hemi-methylated, or fully methylated 42-bp DNA (Fig. 2, F and G). These results indicate that the DNA binding property of GST-Dnmt1 (1–248) is distinct from those reported by Araujo *et al.* (*30*). It seems reasonable that the N-terminal domain showed no specificity for the binding to hemi-methylated DNA, because the N-terminal region (1–290) of Dnmt1 is shown to be dispensable for the specific methylation of hemi-methylated DNA (*32*).

Responsible Region for the DNA Binding Activity—Next we examined the sequence responsible for the DNA binding. We prepared a series of truncated forms of the N-terminal domain of Dnmt1 (Fig. 3A). These truncated proteins (Fig. 3B) were determined the DNA binding activity (Fig. 3C). The DNA binding activity of GST-Dnmt1 (1–290) was similar to that of GST-Dnmt1 (1–343). Dnmt1 (1–290), of which N-terminal GST was removed, bound to DNA in a similar level to that of GST-Dnmt1 (1–290) (supplementary figure S2), indicating that GST did not affect the DNA binding activity. GST-Dnmt1 (1–197), GST-Dnmt1 (119–290), and GST-Dnmt1 (119–197) showed similar amounts of the shifted bands as those of GST-Dnmt1 (1–248) and GST-Dnmt1 (1–343). GST-Dnmt1 (1–146) and GST-Dnmt1 (119–172) showed weak but significant levels of DNA binding activity. Altogether, we concluded that 119–197 is sufficient for the DNA binding activity. The sequences such as 119–146, 147–172 containing PCNA binding motif (160–172) (*9*), and 173–197 was expected to be indispensable for the DNA binding, since not GST-Dnmt1 (1–118) but GST-Dnmt1 (1–146) could bind to DNA, not GST-Dnmt1 (119–146) but GST-Dnmt1 (119–172) bound to DNA, and the DNA binding level of GST-Dnmt1 (119–172) was lower that that of GST-Dnmt1 (1–197). However, neither of the partial sequences of GST-Dnmt1 (119–146), GST-Dnmt1 (147–197), nor GST-Dnmt1 (173–197) by itself could bind to DNA, suggesting that the entire 119–197 sequence may be necessary to form the three dimensional structure for the recognition of DNA.

Amino acids sequences of Dnmt1, deduced from cDNA, have been reported from at least three groups. The N-terminal Dnmt1 (1–343) sequence used in this study was identical to two of them (accession numbers, AF162282 and BC048148). These two sequences give S146V147, while that in the accession number X14805 gives F146 instead. Since the difference resides in the critical positions, we examined the DNA binding activity of the N-terminal domain with F146. The mutated Dnmt1 (1–289) with F146 showed an identical binding activity and specificity to that of Dnmt1 (1–290) with S146V147 (supplementary figure S3).

Mode of DNA Binding of GST-Dnmt1 (119–197)—Different from the report by Fatemi *et al.* (*29*), the N-terminal 1–248 preferred to bind not to the CG containing but to the AT-rich sequence (see Fig. 2, B, C, and D). We further examined the DNA binding activity of GST-Dnmt1 (119–197). GST-Dnmt1 (119–197) bound to 27U as well as 26CG (Fig. 4A), suggesting that the responsible region did not discriminate the CG sequence. Fatemi *et al.* reported that GST-Dnmt1 (1–343) preferentially binds to the CG sequence (*29*), however, even by an identical procedure, a filter binding assay, the binding of GST-Dnmt1 (119–197) towards 26CG was not significantly higher than that towards 26CA, in which a CG sequence was changed to a CA sequence, but preferred to bind to the AT-rich DNA, 26AT (Fig. 4B). To determine the binding specificity of Dnmt1 (119–197) for CG-containing sequence, its binding to 26CG was competed either with 26CG, 26CA, or 26AT (Fig. 4, C and D). The binding was most effectively competed with 26AT, and lesser extent with 26CG or 26CA within a similar range, that is, GST-Dnmt1 (119–197) showed higher binding activity towards 26AT than towards 26CG or 26CA.

The sequence 119–197 responsible for the DNA binding contains two copies of the sequences similar to the AT-hook motif (Fig. 5A), which is known to bind to the minor grove of AT-rich DNA with the consensus sequence of PRGRP (*41*). Since GST-Dnmt1 (119–197) preferred to bind to the AT-rich DNA, we examined the effect of the inhibitors that

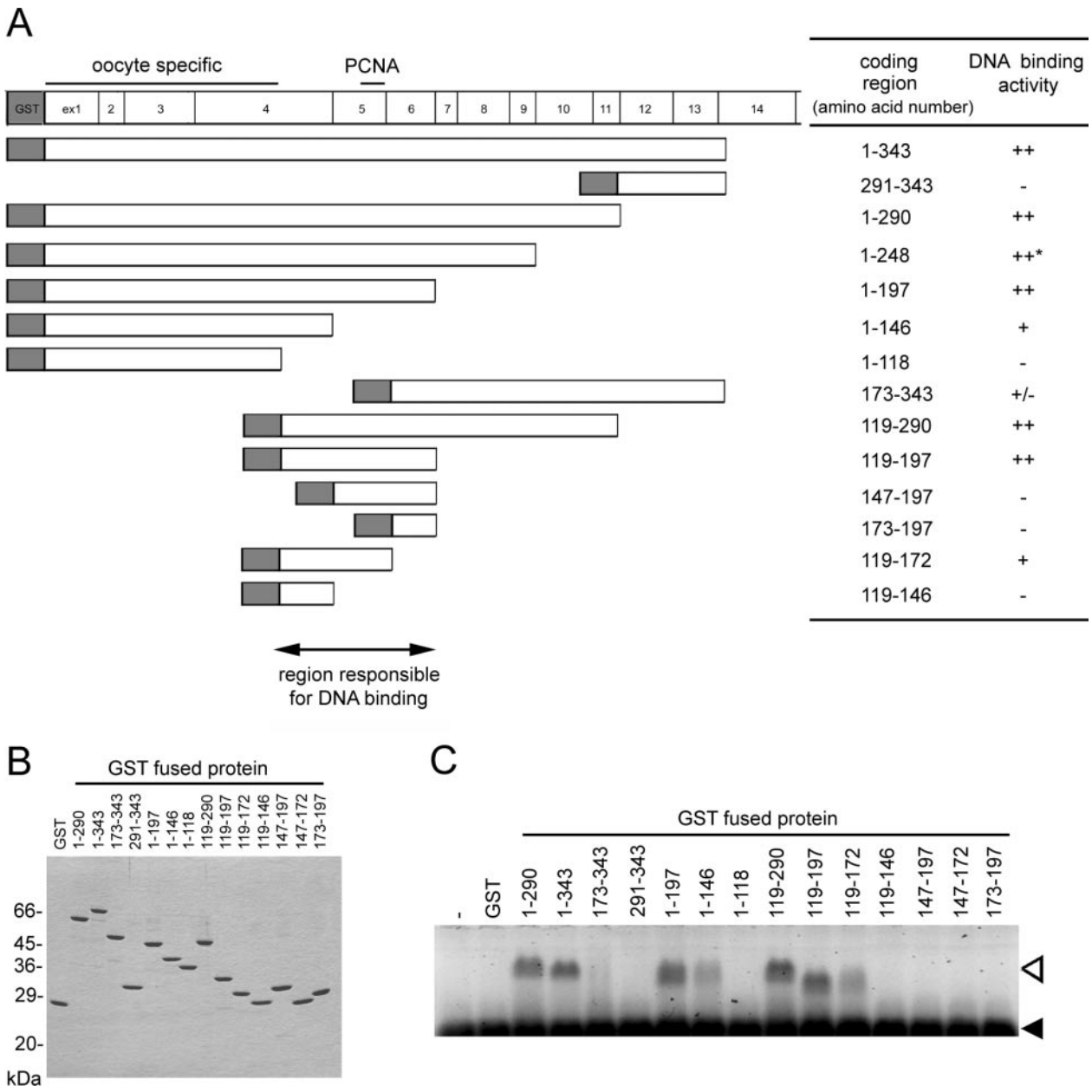

coding region (amino acid number)	DNA binding activity
1-343	++
291-343	-
1-290	++
1-248	++*
1-197	++
1-146	+
1-118	-
173-343	+/-
119-290	++
119-197	++
147-197	-
173-197	-
119-172	+
119-146	-

Fig. 3. **DNA binding sequences in the N-terminal domain.** (A) Schematic illustration of the truncated constructs and their DNA binding activity are summarized. Exon structure, PCNA binding site, and the sequence specifically deleted in the oocyte form are also shown at the top. The narrowed sequence responsible for DNA binding is indicated as horizontal arrow. The relative strength of the DNA binding activities of GST-Dnmt1 (1–248) summarized in the table was taken from Fig. 3C. (B) The purified truncated proteins of the N-terminal region with GST tag at the N-terminus were electrophoresed in a 12% SDS-polyacrylamide gel and stained with CBB. (C) The DNA binding activity of the truncated forms of the N-terminal region was determined by gel shift assay as in Fig. 2B using 26CG as probe. The shifted bands and free probes are indicated by open and closed arrowheads, respectively.

are known to compete with the minor groove binding proteins. As shown in Fig. 5B, distamycin A, which is an anti-tumor drug that binds specifically to the minor groove of AT-rich DNA (*42*), inhibited the DNA binding of GST-Dnmt1 (119–197) to 26AT in a dose-dependent manner (see lanes 3–5). Addition of identical concentrations of distamycin A did not inhibit the binding of GST-Dnmt1 (119–197) to 26CG (Fig. 5C, lanes 3–5). This is due to the preferential binding of distamycin A to the AT-rich sequence. The binding affinity of distamycin A for poly(dG-dC) is two order of magnitude lower than that for poly(dA-dT) (*43*). Another minor groove binding agents, DAPI and netropsin (*44*), also inhibited the DNA binding activity (Fig. 5B, lanes 6–11). On the other hand, methyl green, a major groove binding agent (*45*), did not effectively inhibit the DNA binding activity, (Fig. 5B, lanes 12–14). Similar to the case of distamycin A, addition of identical concentrations of DAPI, netropsin, and methyl green did not inhibit the binding of GST-Dnmt1 (119–197) to 26CG (Fig. 5C, lanes 6–14). Since minor groove binding

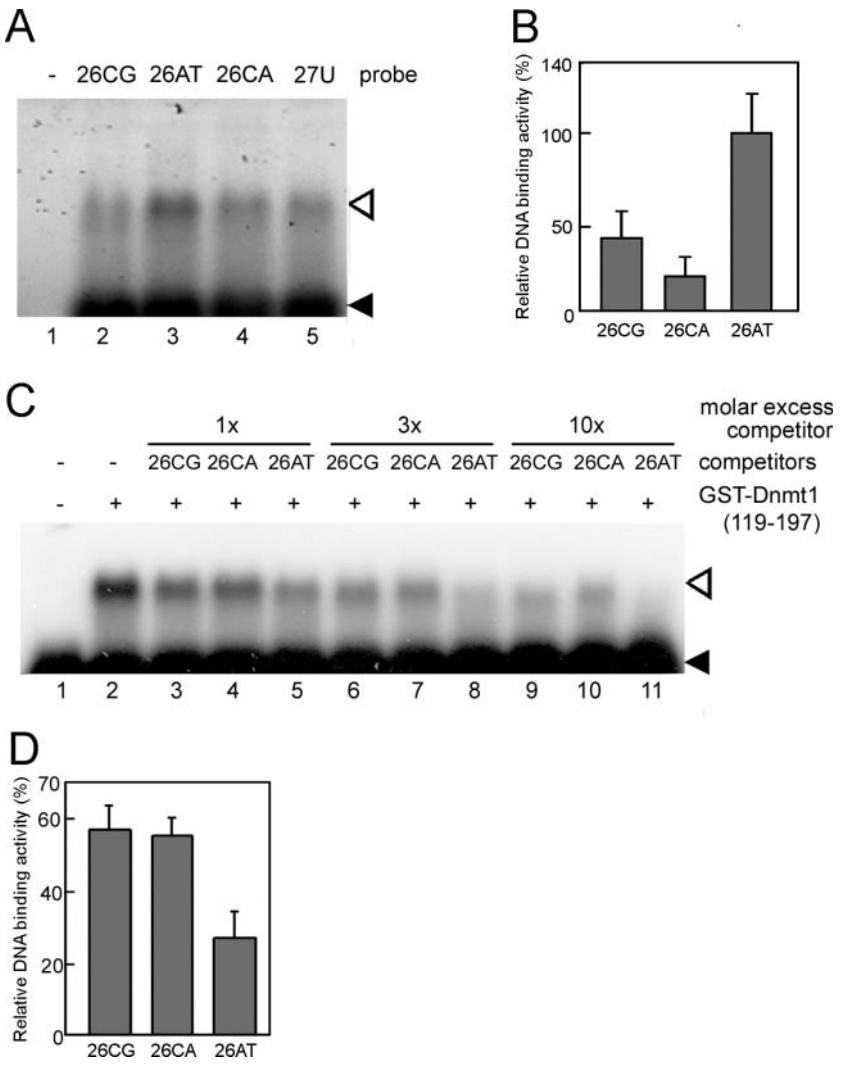

Fig. 4. **DNA binding activity of GST-Dnmt1 (119–197).** (A) The oligonucleotide DNA, 26CG, 26AT, 26CA, or 27U, was incubated with GST-Dnmt1 (119–197), and then the DNA bound to the protein was determined by gel shift assay as in Fig. 2B. (B) DNA binding activity was determined by filter binding assay. Radioactivity was determined and normalized to that of 26AT. The average ± SD obtained from six independent experiments is shown. (C) Radio-labeled 26CG was incubated without (lane 1) or with (lanes 2–11) GST-Dnmt1 (119–197), and no (lanes 1 and 2), one (lanes 3–5), three (lanes 6–8), or ten (lanes 9–11) molar excess non-labeled 26CG (lanes 3, 6, and 9), 26CA (lanes 4, 7, and 10), or 26AT (lanes 5, 8, and 11). The mixtures were electrophoresed as in A, and exposed to X-ray film. (A and C) The shifted bands and free probes are indicated by open and closed arrowheads, respectively. (D) Radio-labeled 26AT and three molar excess of cold 26CG, 26AT, or 26CA were incubated and electrophoresed as in C. The radioactivity of the shifted bands were determined by a BAS2000 and plotted. The average values ± SD were calculated from four independent experiments.

(distamycin A and DAPI) and major groove binding (methyl green) agents have been reported to have similar DNA binding affinities (*43*, *46*, *47*), the results obtained in the present study indicate that the N-terminal domain of Dnmt1 recognizes mainly a minor groove of DNA for the binding.

To examine the contribution of the AT-hook–like motifs in the N-terminal domain for the DNA binding activity, the crucial residues of P and R in the consensus sequence RGRP of the AT-hook motif (*41*) in 126–136 were changed to A and the recombinants were purified (Fig. 5D), and then their DNA binding activity was determined by gel shift assaying (Fig. 5, E and F). When the basic residues were replaced with A, the mutants of R127A, R129A, R133A, and R136A, lost the DNA binding activities, while the P was replaced, the mutants containing P126A, P130A, P132A, and P135A were not affected the DNA binding activity (Fig. 5, E and F). As the consensus sequence of RGRP in the AT-hook motif is not perfectly conserved in the two likely motifs found in the N-terminal domain, which are RSRP and RGPR (see Fig. 5A), the DNA binding mode of the N-terminal domain through 119–197 may not be identical to that of the reported AT-hook motif.

As the sequence 119–197 necessary for the DNA binding contains also the PCNA binding motif at 160–172 (Fig. 3A), it is likely that the sequence responsible for PCNA binding is also involved in the DNA binding activity. To examine this possibility, we next introduced mutations into the PCNA binding motif. Three basic amino acid residues in and near the motif were mutated, i.e., R161A, K171A, and R176A. The mutants of R161A and K171A of GST-Dnmt1 (119–197) lost or decreased the DNA binding activity. On the contrary, the mutant of R176A, of which mutation is out of the PCNA binding motif, did not (Fig. 5, E and F). The sequence responsible for the DNA binding covers the PCNA binding site. Thus, not only the AT-hook–like sequences but also the PCNA binding motif was involved in the DNA recognition either directly or indirectly.

PCNA Competes with DNA for the Binding to the N-Terminal Domain of Dnmt1—Since the sequence responsible for the DNA binding in the N-terminal domain of Dnmt1 was extended to that for PCNA binding, we next determined whether or not the binding of the N-terminal domain of Dnmt1 to DNA interferes with that to PCNA. Under the examined conditions, PCNA alone did not show any shifted band (Fig. 6C, lanes 2–4). PCNA might run off

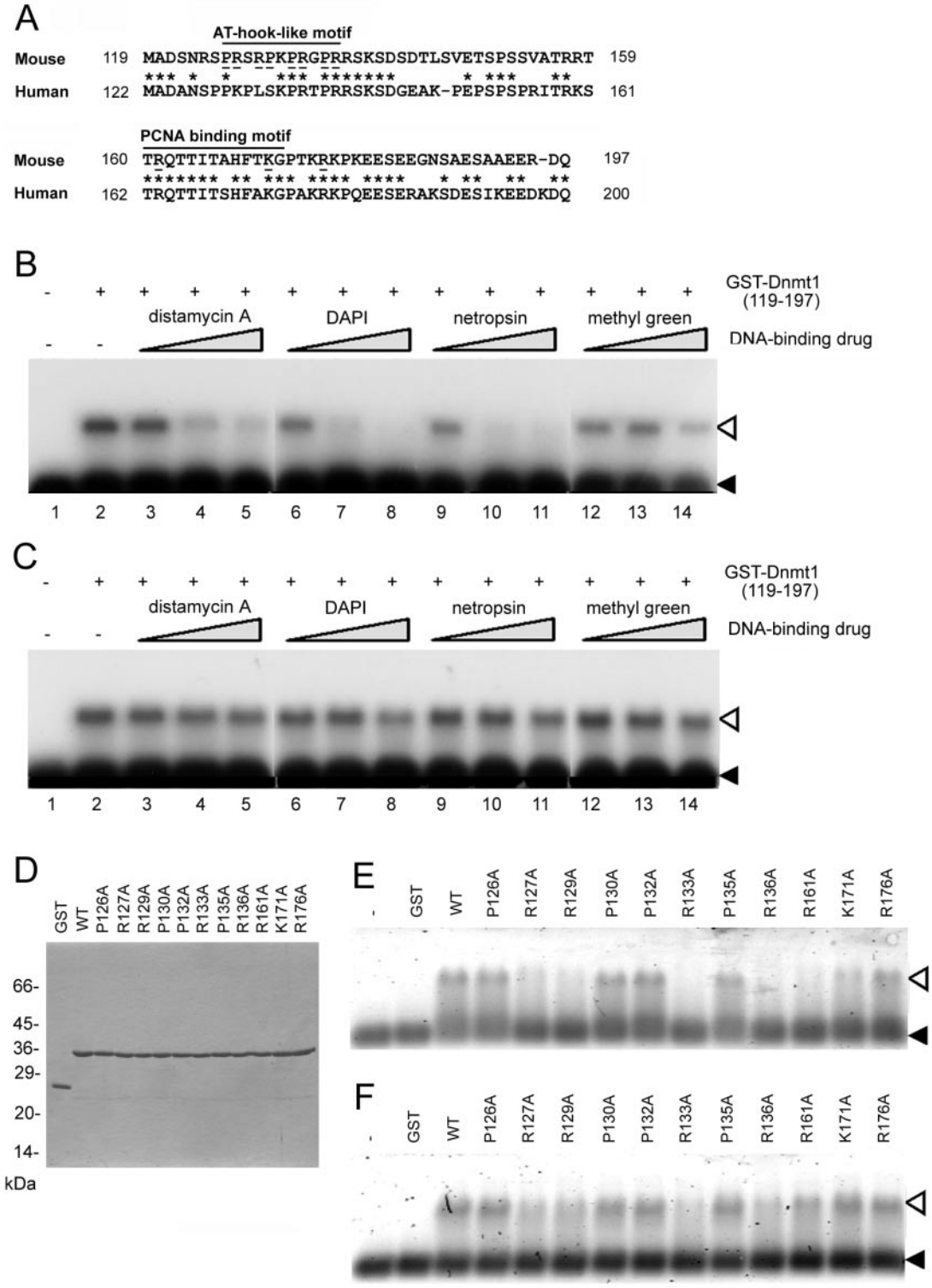

Fig. 5. **Effects of the drugs and mutations on the DNA binding activity of Dnmt1 (119–197).** (A) The mouse DNA binding sequence 119–197 is aligned with the corresponding human sequence. The amino acid residues identical between mouse and human were indicated as asterisks. The sequence homologous to the AT-hook motif and PCNA binding sequence are indicated. The mutated amino acid residues are indicated by underline. (B) Radio-labeled 26AT and GST-Dnmt1 (119–197) were incubated in the presence of 0.1, 1, and 10 μM distamycin A (lanes 3–5), DAPI (lanes 6–8), netropsin (lanes 9–11), or methyl green (lanes 12–14). The DNA bound to the protein was determined by gel shift assay as in Fig. 2C. (C) Radio-labeled 26CG and GST-Dnmt1 (119–197) were incubated and analyzed as in B. (D) CBB staining of GST, GST-Dnmt1 (119–197), and the GST-Dnmt1 (119–197) mutated at indicated positions (2 μg protein each) were electrophoresed in a 12% SDS-polyacrylamide gel. (E and F) DNA binding activities of GST, wild-type GST-Dnmt1 (119–197), and its mutants were determined as in Fig. 2B using the oligonucleotide DNA 26CG (E) and 26AT (F) as probes. (B, C, E, and F) The shifted bands and free probes are indicated by open and closed arrowheads, respectively.

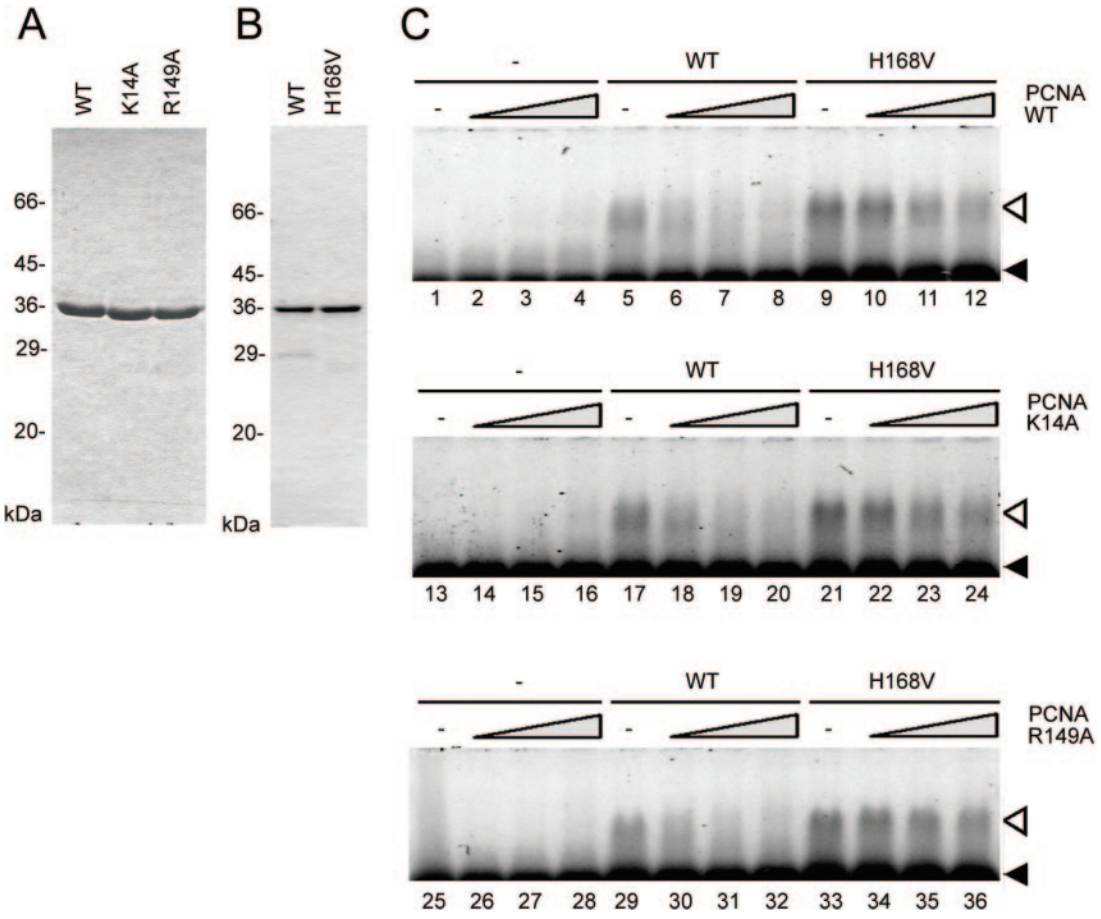

Fig. 6. **Effect of PCNA on the DNA binding activity of the N-terminal domain of Dnmt1.** Wild-type (WT) and mutant PCNA (K14A and R149A) (A), and GST-Dnmt1 (119–197) (WT) and mutant GST-Dnmt1 (119–197) at H168V (H168V) (B) were electrophoresed in a 12% SDS–polyacrylamide gel, and stained with CBB. Two micrograms proteins were loaded in each lane. (C) GST-Dnmt1 (119–197) (lanes 5–8, 17–20, and 29–32) or GST-Dnmt1 (119–197) H168V (lanes 9–12, 21–24, and 33–36) (5 pmol protein each) was mixed with oligonucleotide DNA, 26CG, in the absence (lanes 1, 5, 9, 13, 17, 21, 25, 29, and 33) or the presence of 5.1 pmol (lanes 2, 6, 10, 14, 18, 22, 26, 30, and 34), 15 pmol (lanes 3, 7, 11, 15, 19, 23, 27, 31, and 35), or 45 pmol (lanes 4, 8, 12, 16, 20, 24, 28, 32, and 36) of PCNA. The reaction mixture was analyzed as in Fig. 2B. The shifted band and free probes are indicated by open and closed arrowheads, respectively.

from the linear DNA used in the binding assay, though PCNA is known to bind to DNA (*33*). The addition of PCNA to the reaction mixtures decreased the shifted bands composed of the DNA and GST-Dnmt1 (119–197) in a dose dependent manner (Fig. 6C, lanes 5–8). However, the addition of PCNA to the Dnmt1 (119–197) with a mutation at H168V, which cannot bind to PCNA (*9*), scarcely affected the DNA binding activity (Fig. 6C, lanes 9–12). The result indicates that the binding of Dnmt1 (119–197) to the PCNA competed with that to the DNA. To further confirm that the inhibitory effect of PCNA on the binding of Dnmt1 (119–197) to DNA is not through the DNA binding activity of PCNA but a direct effect on Dnmt1, the mutants of PCNA with K14A and R149A that lack DNA binding activity (*33*) were employed. The addition of these PCNA mutants also inhibited the DNA binding activity of Dnmt1 (119–197) to a similar level as to that of wild-type PCNA (Fig. 6C, lanes 17–20 and 29–32). Altogether, it can be concluded that the binding of Dnmt1 (119–197) to DNA was directly competed with that to PCNA through the common binding sequence in Dnmt1 (119–197).

Next, the effect of the addition of DNA on the direct interaction between the N-terminal domain of Dnmt1 and PCNA was determined. Wild-type PCNA was pulled down with the glutathione-Sepharose bound to GST-Dnmt1 (119–197) in the absence of DNA (Fig. 7, upper left panel, 0× DNA), supporting the previous report that Dnmt1 binds to PCNA (*9*). PCNA with mutations in the residues responsible for DNA binding (K14A and R149A shown at left middle and lower panels) also bound to GST-Dnmt1 (119–197) in the absence of DNA. The amount of all types of PCNA bound to GST-Dnmt1 (119–197) was decreased by the addition of DNA in a dose dependent manner (Fig. 7, left panels, 3× and 10× DNA). These results support the conclusion that PCNA and DNA binding to the N-terminal 119–197 of Dnmt1 directly competes.

DISCUSSION

The N-Terminal 1–248 Forms a Domain Structure—In the present study, we found that the N-terminus of Dnmt1 (1–248), encoded by exon 1–9, forms a domain structure. Margot et al. have concluded that Dnmt1 molecule is

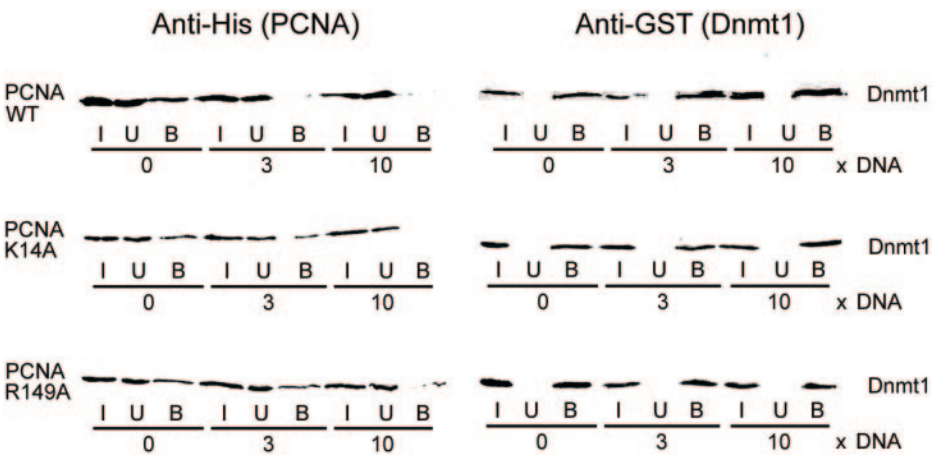

Fig. 7. **Effect of DNA on the PCNA binding activity of the N-teminal domain of Dnmt1.** Glutathione-Sepharose bound with 60 pmol of Dnmt1 (119–197) were mixed with equal mol of His-tagged PCNA in the absence or presence of 3 and 10 molar excess (× DNA) oligonucleotide DNA, 26CG. As for PCNA, wild type (upper panel), K14A (middle panel), and R149A (lower panel) were used. PCNA and Dnmt1 of input (I), matrix bound (B), and unbound (U) fractions were determined by Western blotting by anti–His-tag antibodies (left panels) and anti-GST antibodies (right panels).

constituted of three separable domain structures, *i.e.*, the N-terminal, 1–352 encoded in exon 1–14, the middle part containing zinc finger-like and polybromo-1 homology domains, and the C-terminal catalytic region, according to the sequence homology alignment and exon arrangement analyses of the Dnmt1 deduced in several species (*28*). The sequence comprising N-terminal domain identified in the present study did not completely match with that reported by Margot *et al.* (*28*). Due to our biochemical results, the core N-terminal domain is likely to be 1–248.

Even when the N-terminal domain was deleted, the Dnmt1 neither changes its specific activity nor the specificity towards hemi-methylated DNA substrate (*32*). The N-terminal domain is dispensable for the hemi-methylated DNA methylating activity of Dnmt1. However, the N-terminal domain (1–248) is reported to associate with PCNA, which is a prerequisite factor for replication and repair (*33*), and Dnmt1 is recruited to the PCNA existing sites (*8–12*), expected to fully methylate the newly synthesized hemi-methylated CG sites. In addition, the N-terminal domain interacts with DMAP1 and HDAC2, which are the factors involved in gene silencing (*20*). Furthermore, the N-terminal domain binds another DNA methyltransferases Dnmt3a and Dnmt3b, which are reported to create DNA methylation patterns during embryogenesis and in germ cells (*23*). Since the fidelity of Dnmt1 itself to maintain DNA methylation patterns during replication is low (*32*, *48*) compared to that under physiological conditions (*49*), the interaction of Dnmt1 with these *de novo*–type DNA methyltransferases, possibly Dnmt3b, may help in maintaining the DNA methylation patterns (*50*, *51*). Therefore, it is rational to speculate that the N-terminal domain is working as a platform for the interaction with those factors that regulate the function and localization of Dnmt1 (Fig. 1F).

The DNA Binding Activity of the N-Terminal Domain—The sequence responsible for DNA binding in the N-terminal domain was narrowed to 79 amino acid residues, which harbors AT-hook–like sequences and PCNA binding motif. The domain preferred to bind to the minor groove of AT-rich sequence (Figs. 4 and 5), and did not discriminate the CG sequence and methylation status (Figs. 2 and 4). These properties of the N-terminal domain do not go along with the previous report that the N-terminal 1–343 favors to bind CG containing DNA (*29*). One reason for the discrepancy could be due to the oligonucleotide sequence used for the binding study. To determine the preferential binding towards the CG sequence, a single CG site in the probe 26CG was changed to CA in 26CA in the present study (see Table 1). On the other hand, Fatemi et al. changed not only a CG site in the 30 base pair oligonucleotide but also the flanking three nucleotides (*29*). This adjacent nucleotide change might have affected the binding activity of the N-terminal domain of Dnmt1. Furthermore, it was reported by another group that the DNA binding sequence (amino acid residues 122–417) including PCNA binding motif, which is located in human Dnmt1 (162–174), recognizes hemi-methylated CG (*30*). In their report, hemi-methylated hairpin oligonucleotide DNA was used for the binding assay. As Dnmt1 specifically recognizes the edge of fold backed single stranded DNA (*52*, *53*), the N-terminal domain might recognize such the unusual structure other than hemi-methylated double stranded DNA when hairpin oligonucleotide DNA is used. It may not be reasonable to assume that the DNA binding site near PCNA binding motif is contributing to the recognition of hemi-methylated CG, since the region including PCNA binding site is shown to be dispensable for the hemi-methylated DNA methylating activity of Dnmt1 (*32*).

Possible Function of the DNA Binding Activity in N-Terminal Domain—Since the N-terminal domain identified in the present study preferred to bind an AT-rich sequence, Dnmt1 could be accumulated at AT-rich sites such that the LINE-1 repetitive sequence (*54*), satellite DNA (*55*), and many of the promoters of tissue-specific genes (*56*). These sequences, though CG sequences are infrequent, are highly methylated, except for the promoters of tissue-specific genes in expressing cells (*40*, *57*, *58*). Maintenance of the methylation of these regions is quite important. Methylation of the promoters of tissue-specific genes in non-expressing cells ensures a normal differentiation state of the cells. The LINE-1 repeat becomes hypomethylated in cancer cells, and hypomethylation of the satellite DNA could be a trigger for carcinogenesis in man (*59–61*). It is likely that the location of Dnmt1 contributes to the maintenance of the methylation status in these regions.

The DNA binding activity of the N-terminal domain identified in the present study competed with the PCNA

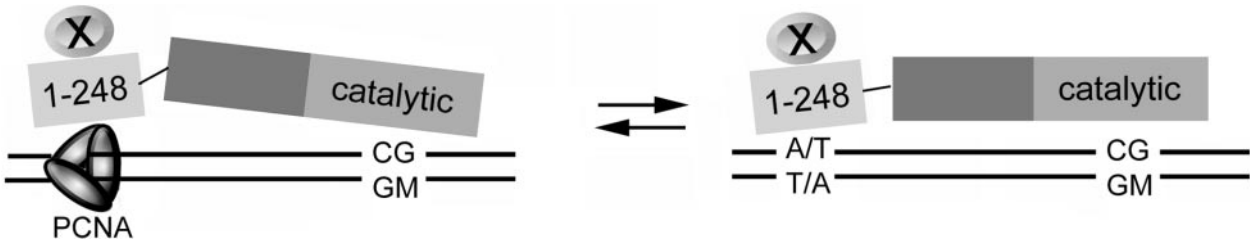

Fig. 8. **Schematic illustration of the localization of Dnmt1 through the N-terminal domain.** The DNA and PCNA binding activity of the N-terminal domain deduced from this study were schematically illustrated. The N-terminal region also associated other protein (X) as summarized in Fig. 1F. During replication and long-patch BER, Dnmt1 interact with PCNA and methylates the hemimethylated CpG (CG/GM) that appears during the synthesis of DNA strand to maintain the methylation patterns (A). During non–S-phase, Dnmt1 may localize on the AT-rich DNA without interacting with PCNA. This localization may contribute to restoration of the methylation patterns that are hemi-demethylated by short-patch BER during non–S-phase (B).

binding. This means that Dnmt1 bound to DNA through the N-terminal domain cannot bind PCNA, and, *vice versa*, Dnmt1 bound to PCNA cannot directly bind to DNA through the N-terminal domain (Fig. 8). Although the expression of Dnmt1 is highest at S phase, it is also detectable at G2 and M phases, at which phases Dnmt1 associates preferentially with heterochromatin (*10*). The methylated cytosine residue prone to undergo spontaneous deamination, and the resulting G/T mismatch is corrected by a base excision repair (BER) pathway. BER in mammalian cells occurs by two pathways termed "short-patch" or single-nucleotide replacement and "long-patch" or several-nucleotide replacement BER (*62*). The short-patch BER is accomplished by DNA polymerase β without a help of PCNA, and this newly repaired base pair becomes hemi-methylated CpG. To recover this hemi-methylated state to fully methylated form, Dnmt1 should be recruited to the site. The DNA binding activity of the N-terminal domain may contribute in locating Dnmt1 at such the hemi-methylated CpG that is produced replication-independent manner at non-S phase.

Supplementary figures available as figures S1–S3.

This work was supported by Grants-in-Aid for Scientific Research (B) and for Young Scientists from the JSPS (IS), and the National Project on Protein Structural and Functional Analyses.

REFERENCES

1. Antequera, F. and Bird, A. (1993) CpG islands in DNA methylation in *Molecular Biology and Biological Significance* (Jost, J.P. and Saluz, H.P., eds.) pp. 169–185, Birkhäuser Verlag, Basel
2. Ehrlich, M., Gama-Sosa, M.A., Huang, L.H., Midgett, R.M., Kuo, K.C., McCune, R.A., and Gehrke, C. (1982) Amount and distribution of 5-methylcytosine in human DNA from different types of tissues of cells. *Nucleic Acids Res.* **10**, 2709–2721
3. Okano, M., Bell, D.W., Haber, D.A., and Li, E. (1999) DNA methyltransferases Dnmt3a and Dnmt3b are essential for de novo methylation and mammalian development. *Cell* **99**, 247–257
4. Kaneko-Ishino, T., Kohda, T., and Ishino, F. (2003) The regulation and biological significance of genomic imprinting in mammals. *J. Biochem.* **133**, 699–711
5. Laird, P.W. and Jaenisch, R. (1996) The role of DNA methylation in cancer genetic and epigenetics. *Annu. Rev. Genet.* **30**, 441–464
6. Bird, A. (2002) DNA methylation patterns and epigenetic memory. *Genes Dev.* **16**, 6–21
7. Monk, M. (1990) Changes in DNA methylation during mouse embryonic development in relation to X-chromosome activity and imprinting. *Philos. Trans. R. Soc. Lond. B Biol. Sci.* **326**, 299–312
8. Leonhardt, H., Page, A.W., Weier, H.U., and Bestor, T.H. (1992) A targeting sequence directs DNA methyltransferase to sites of DNA replication in mammalian nuclei. *Cell* **71**, 865–873
9. Chuang, L.S., Ian, H.I., Koh, T.W., Ng, H.H., Xu, G., and Li, B.F. (1997) Human DNA-(cytosine-5) methyltransferase-PCNA complex as a target for p21WAF1. *Science* **277**, 1996–2000
10. Easwaran, H.P., Schermelleh, L., Leohardt, H., and Cardoso, M.C. (2004) Replication-independent chromatin loading of Dnmt1 during G2 and M phases *EMBO Reports* **5**, 1181–1186
11. Iida, T., Suetake, I., Tajima, S., Morikawa, H., Ohta, S., Obuse, C., and Tsurimoto, T. (2002) PCNA clamp facilitates action of DNA cytosine methyltransferase 1 on hemimethylated DNA. *Genes Cells* **7**, 997–1007
12. Mortusewicz, O., Schermelleh, L., Walter, J., Cardoso, M.C., and Leonhardt, H. (2005) Recruitment of DNA methyltransferase I to DNA repair sites. *Proc. Natl. Acad. Sci. USA* **102**, 8905–8909
13. Li, E., Betor, T.H., and Jaenisch, R. (1992) Targeted mutation of the DNA methyltransferase gene results in embryonic lethality. *Cell* **69**, 915–926
14. Bestor, T.H. (1992) Activation of mammalian DNA methyltransferase by cleavage of a Zn binding regulatory domain. *EMBO J.* **11**, 2611–2617
15. Bestor, T., Laudano, A., Mattaliano, R., and Ingram, V. (1988) Cloning and sequencing of a cDNA encoding DNA methyltransferase of mouse cells. The carboxyl-terminal domain of the mammalian enzymes is related to bacterial restriction methyltransferases. *J. Mol. Biol.* **203**, 971–983
16. Yen, R, W., Vertino, P, M., Nelkin, B, D., Yu, J, J., el-Deiry, W., Cumaraswamy, A., Lennon, G, G., Trask, B, J., Celano, P., and Baylin, S, B. (1992) Isolation and characterization of the cDNA encoding human DNA methyltransferase. *Nucleic Acids Res.* **20**, 2287–2291
17. Tajima, S., Tsuda, H., Wakabayashi, N., Asano, A., Mizuno, S., and Nishimori, K. (1995) Isolation and expression of a chicken DNA methyltransferase cDNA. *J. Biochem.* **117**, 1050–1057
18. Aniello, F., Locascio, A., Fucci, L., Geraci, G., and Branno, M. (1996) Isolation of cDNA clones encoding DNA methyltransferase of sea urchin P. lividus: expression during embryonic development. *Gene* **178**, 57–61
19. Kimura, H., Ishihara, G., and Tajima, S. (1996) Isolation and expression of a *Xenopus laevis* DNA methyltransferase cDNA. *J. Biochem.* **120**, 1182–1189

20. Rountree, M.R., Bachman, K.E., and Baylin, S.B. (2000) DNMT1 binds HDAC2 and a new co-repressor, DMAP1, to form a complex at replication foci. *Nat. Genet.* **25**, 269–277
21. Fuks, F., Burgers, W.A., Brehm, A., Hughes-Davies, L., and Kouzarides, T. (2000) DNA methyltransferase Dnmt1 associates with histone deacetylase activity. *Nat. Genet.* **24**, 88–91
22. Robertson, K.D., Ait-Si-Ali, S., Yokochi, T., Wade, P.A., Jones, P.L., and Wolffe, A.P. (2000) DNMT1 forms a complex with Rb, E2F1 and HDAC1 and represses transcription from E2F-responsive promoters. *Nat. Genet.* **25**, 338–342
23. Pradhan, S. and Kim, G.D. (2002) The retinoblastoma gene product interacts with maintenance human DNA (cytosine-5) methyltransferase and modulates its activity. *EMBO J.* **21**, 779–788
24. Kimura, H. and Shiota, K. (2003) Methyl-CpG-binding protein, MeCP2, is a target molecule for maintenance DNA methyltransferase, Dnmt1. *J. Biol. Chem.* **278**, 4806–4812
25. Fuks, F., Hurd, P.J., Deplus, R., and Kouzarides, T. (2003) The DNA methyltransferases associate with HP1 and the SUV39H1 histone methyltransferase. *Nucleic Acids Res.* **31**, 2305–2312
26. Estéve, P.O., Chin, H.G., and Pradhan, S. (2005) Human maintenance DNA (cytosine-5)-methyltransferase and p53 modulate expression of p53-repressed promoters. *Proc. Natl. Acad. Sci. USA* **102**, 1000–1005
27. Kim, G.D., Ni, J., Kelesoglu, N., Roberts, R.J., and Pradhan, S. (2002) Co-operation and communication between the human maintenance and de novo DNA (cytosine-5) methyltransferases. *EMBO J.* **21**, 4183–4195
28. Margot, J.B., Aguirre-Arteta, A.M., Giacco, B.V., Pradhan, S., Roberts, R.J., Cardoso, M.C., and Leohardt, H. (2000) Structure and function of the mouse DNA methyltransferase gene: Dnmt1 shows a tripartite structure. *J. Mol. Biol.* **297**, 293–300
29. Fatemi, M., Hermann, A., Pradhan, S., and Jeltsch, A. (2001) The activity of the murine DNA methyltransferase Dnmt1 is controlled by interaction of the catalytic domain with the N-terminal part of the enzyme leading to an allosteric activation of the enzyme after binding to methylated DNA. *J. Mol. Biol.* **309**, 1189–1199
30. Araujo, F.D., Croteau, S., Slack, A.D., Milutinovic, S., Bigey, P., Price, G.B., Zannis-Hajopoulos, M., and Szyf, M. (2001) The DNMT1 target recognition domain resides in the N terminus. *J. Biol. Chem.* **276**, 6930–6936
31. Pradhan, S. and Estéve, P.O. (2003) Allosteric activator domain of maintenance human DNA (cytosine-5) methyltransferase and its role in methylation spreading. *Biochemistry* **42**, 5321–5332
32. Vilkaitis, G., Suetake, I., Klimašauskas, S., and Tajima, S. (2005) Processive methylation of hemimethylated CpG sites by mouse Dnmt1 DNA methyltransferase. *J. Biol. Chem.* **280**, 64–72
33. Fukuda, K., Morioka, H., Imajou. S., Ikeda, S., Ohtsuka, E., and Tsurimoto, T. (1995) Structure-function relationship of the eukaryotic DNA replication factor, proliferating cell nuclear antigen. *J. Biol. Chem.* **270**, 22527–22534
34. Sanger, F., Nicklen, S., and Coulson, A.R. (1977) DNA sequencing with chain-terminating inhibitors. *Proc. Natl. Acad. Sci. USA* **74**, 5463–5467
35. Suetake, I., Shinozaki, F., Miyagawa, J., Takeshima, H., and Tajima, S. (2004) DNMT3L stimulates the DNA methylation activity of Dnmt3a and Dnmt3b through a direct interaction. *J. Biol. Chem.* **279**, 27816–27823
36. Laemmli, U.K. (1970) Cleavage of structural proteins during the assembly of the head of bacteriophage T4. *Nature* **227**, 680–685
37. Suetake, I., Tajima, S., and Asano, A. (1995) A novel DNA binding protein that recognizes the methylated c-Myc binding motif. *J. Biochem.* **118**, 244–249
38. Suetake, I., Shi, L., Watanabe, D., Nakamura, M., and Tajima, S. (2001) Proliferation stage-dependent expression of DNA methyltransferase (Dnmt1) in mouse small intestine. *Cell Struct. Funct.* **26**, 79–86
39. Mertineit, C., Yoder, J.A., Taketo, T., Laird, D.W., Trasler, J.M., and Bestor, T.H. (1998) Sex-specific exons control DNA methyltransferase in mammalian germ cells. *Development* **125**, 889–897
40. Tajima, S. and Suetake, I. (1998) Regulation and funcztion of DNA methylation in vertebrates. *J. Biochem.* **123**, 993–999
41. Reeves, R. (2001) Molecular biology of HMGA proteins: hubs of nuclear function. *Gene* **277**, 63–81
42. Coll, M., Frederick, C.A., Wang. A.H., and Rich, A. (1987) A bifurcated hydrogen-bonded conformation in the d(A.T) base pairs of the DNA dodecamer d(CGCAAATTTGCG) and its complex with distamycin. *Proc. Natl. Acad. Sci. USA* **84**, 8385–8389
43. Bartulewicz, D., Bielawski, K., and Bielawska, A. (2002) Carbocyclic analogues of netropsin and distamycin: DNA-binding properties and inhibition of DNA topoisomerases. *Arch. Pharm. (Weinheim)* **335**, 422–426
44. Geierstanger, B.H. and Wemmer, D.E. (1995) Complexes of the minor groove of DNA. *Annu. Rev. Biophys. Biomol. Struct.* **24**, 463–493
45. Kim, S.K. and Nordén, B. (1993) Methyl green. A DNA major-groove binding drug. *FEBS Lett.* **315**, 61–64
46. Kumar, K.A. and Muniyappa, K. (1992) Use of structure-directed DNA ligands to probe the binding of recA protein to narrow and wide grooves of DNA and on its ability to promote homologous pairing. *J. Biol. Chem.* **267**, 24824–24832
47. Tuite, E., Sehlstedt, U., Hagmar, P., Nordén, B., and Takahashi, M. (1997) Effects of minor and major groove-binding drugs and intercalators on the DNA association of minor groove-binding proteins RecA and deoxyribonuclease I detected by flow linear dichroism. *Eur. J. Biochem.* **243**, 482–492
48. Laird, C.D., Pleasant, N.D., Clark, A.D., Sneeden, J.L., Hassan, K.M., Manley, N.C., Vary, J.C. Jr., Morgan, T., Hansen, R.S., and Stöger, R. (2004) Hairpin-bisulfite PCR: assessing epigenetic methylation patterns on complementary strands of individual DNA molecules. *Proc. Natl. Acad. Sci. USA* **101**, 204–209
49. Ushijima, T., Watanabe, N., Okochi, E., Kaneda, A., Sugimura, T., Miyamoto, K. (2003) Fidelity of the methylation pattern and its variation in the genome. *Genome Res.* **13**, 868–874
50. Chen, T., Ueda, Y., Dodge, J.E., Wang, Z., and Li, E. (2003) Establishment and maintenance of genomic methylation patterns in mouse embryonic stem cells by Dnmt3a and Dnmt3b. *Mol. Cell. Biol.* **23**, 5594–5605
51. Datta, J., Ghoshal, K., Sharma, S.M., Tajima, S., and Jacob, S.T. (2003) Biochemical fractionation reveals association of DNA methyltransferase (Dnmt) 3b with Dnmt1 and that of Dnmt 3a with a histone H3 methyltransferase and Hdac1. *J. Cell. Biochem.* **88**, 855–64
52. Smith, S.S., Lingeman, R.G., and Kaplan, B.E. (1992) Recognition of foldback DNA by the human DNA (cytosine-5-)-methyltransferase. *Biochemistry* **31**, 850–854
53. Christman, J.K., Sheikhnejad, G., Marasco, C.J., and Sufrin, J.R. (1995) 5-Methyl-2′-deoxycytidine in single-stranded DNA can act in cis to signal *de novo* DNA methylation. *Proc. Natl. Acad. Sci. USA* **92**, 7347–7351
54. Deininger, P.L., Moran, J.V., Batzer, M.A., and Kazasian, H.H., Jr. (2003) Mobile elements and mammalian genome evolution. *Curr. Opin. Genet. Dev.* **13**, 651–658
55. Hörz, W. and Altenburger, W. (1981) Nucleotide sequence of mouse satellite DNA. *Nucleic Acids Res.* **9**, 683–696
56. Schug, J., Schuller, W.P., Kappen, C., Salbaum, J.M., Bucan, M., and Stoeckert, C.R., Jr. (2005) Promoter features related to tissue specificity as measured by Shannon entropy. *Genome Biol.* **6**, R33

57. Yoder, J.A., Walsh, C.P., and Bestor, T.H. (1997) Cytosine methylation and the ecology of intragenomic parasites. *Trends Genet.* **13**, 335–340
58. Ponzetto-Zimmerman, C. and Wolgemuth, D.J. (1984) Methylation of satellite sequences in mouse spermatogenic and somatic DNAs. *Nucleic Acids Res.* **12**, 2807–2822
59. Ushijima, T., Morimura, K., Hosoya, Y., Okonogi, H., Tatematsu, M., Sugimura, T., and Nagao, M. (1997) Establishment of methylation-sensitive-representational difference analysis and isolation of hypo- and hypermethylated genomic fragments in mouse liver tumors. *Proc. Natl. Acad. Sci. USA* **94**, 2284–2289
60. Ehrlich, M., Hopkins, N.E., Jiang, G., Dome, J.S., Yu, M.C., Woods, C.B., Tomlinson, G.E., Chintagumpala, M., Champagne, M., Dillerge, L., Parham, D.M., and Sawyer, J. (2003) Satellite DNA hypomethylation in karyotyped Wilms tumors. *Cancer Genet. Cytogenet.* **141**, 97–105
61. Wong, N., Lam, W.C., Lai, P.B., Pang, E., Lau, W.Y., and Johnson, P.J. (2001) Hypomethylation of chromosome 1 heterochromatin DNA correlates with q-arm copy gain in human hepatocellular carcinoma. *Am. J. Pathol.* **159**, 465–471
62. Wilson, S.H. (1998) Mammalian base excision repair and DNA polymerase beta. *Mut. Res.* **403**, 207–215